Urol Res (1987) 15:67–73

Urological Research

Stone Formation in Human Kidney

F. Hering[1], Th. Briellmann[2], G. Lüönd[3], H. Guggenheim[3], H. Seiler[2] and G. Rutishauser[1]

[1]Urologische Klinik, Departement für Chirurgie der Universität, Kantonsspital Basel
[2]Institut für Anorganische Chemie and [3]Geologisch-paläontologisches Institut, Universität Basel, Basel, Switzerland

Accepted: January 1, 1987

Summary. Microscopic crystals were found by SEM analysis in kidneys of stone forming patients as well as in kidneys of non-stone formers. In most samples calcifications were intratubular in the collecting ducts near the papillary tip. 1–2 μm sized particles lay in a gelatinous substance on the epithelium. The only difference in crystal composition is the higher phosphate content in the kidneys of the non-stone forming group. A correlation between the element concentration of the tissue and the occurrence of microliths is given by the cadmium content of the kidney samples. Both groups showed higher cadmium values in the cortex or medulla when crystals were found in the corresponding papillary samples. Urine supersaturation with respect to calcium oxalate was higher in the stone forming group caused by a higher calcium and oxalate but a lower magnesium excretion.

Key words: Microliths, Crystallisation site, Cadmium concentration in kidney.

Introduction

In 1985 we presented some preliminary results [1], since then 10 kidneys from stone fromers and 18 kidneys of patients free from stone disease were analysed. The aim of the study was to reveal sites and types of sub-microscopic calcifications and to study their correlation to tissue- and to urine concentrations.

Methods

Immediately after nephrectomy the kidneys were divided into wedge sections containing cortex, medulla and papilla. One part of these samples was used for scanning electron microscopy (SEM), the other part for chemical analysis of sodium, potassium, magnesium, calcium, zinc, copper, cadmium and lead in the tissue.

Before surgery a 12 h-urine was collected from each patient in which the concentrations of sodium, potassium, calcium, magnesium, phosphate, uric acid, oxalate, citrate, as well as pH and volume were determined. Urine supersaturation was calculated by Finlayson's EQUIL 1 program [2].

Results

Scanning Electron Microscopy

Microscopic crystals were found above all in the collecting ducts near the papillary tip and in some cases in the outer medulla zone. We were surprised by the fact that "microliths" were also detectable in kidneys of non-stone formers. Figure 1 shows a 1 μm spheroidal crystal in a niche of the collecting duct (kidney excised due to hypernephroma).

In another collecting duct of the same kidney spheroidal crystals appear again which are embedded in a gelatinous substance and seem thereby to be fixed (Fig. 2, 3). Morphologically similar crystallisations are of course also found in kidneys of stone formers (Fig. 4, 5). The surface of these crystals is composed of a great number of small spheroidal particles.

When the calcium concentration is measured along a line (Fig. 6) by line scan analysis a distinct calcium peak can only be observed in the microcrystal and not in the surrounding tissue or in the tubular walls. Due to the preparation the tissue analysis permits only approximate values. The samples were coated with silver to enable a good phosphate EDAX point analysis (Fig. 7).

Non-stone formers differed from the stone forming group in the phosphate content of their microcrystals. In Fig. 8 several collecting ducts of a non-stone bearing patient are shown in a diagonal section. In Fig. 9 a collecting duct loaded with cobble-stone shaped crystals can be seen. The EDAX point analysis in one of these particles gave a phosphate peak even higher than the calcium peak (Fig. 10); this feature was evident in almost all kidneys of non-stone bearing patients.

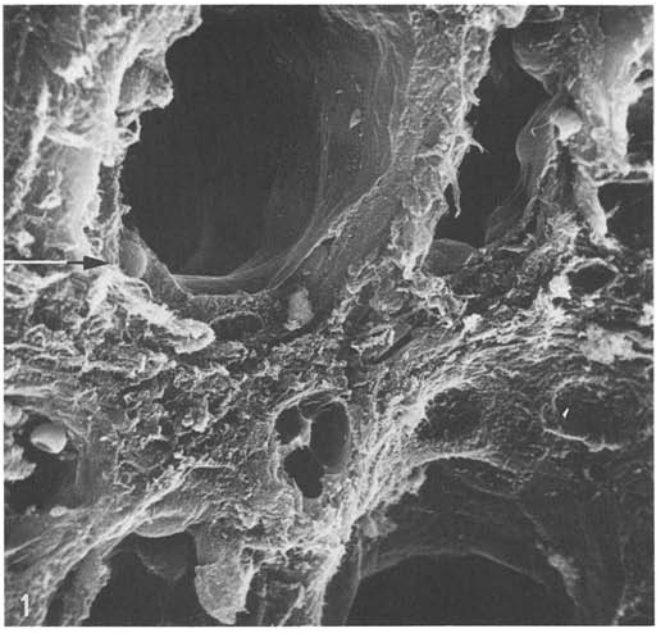

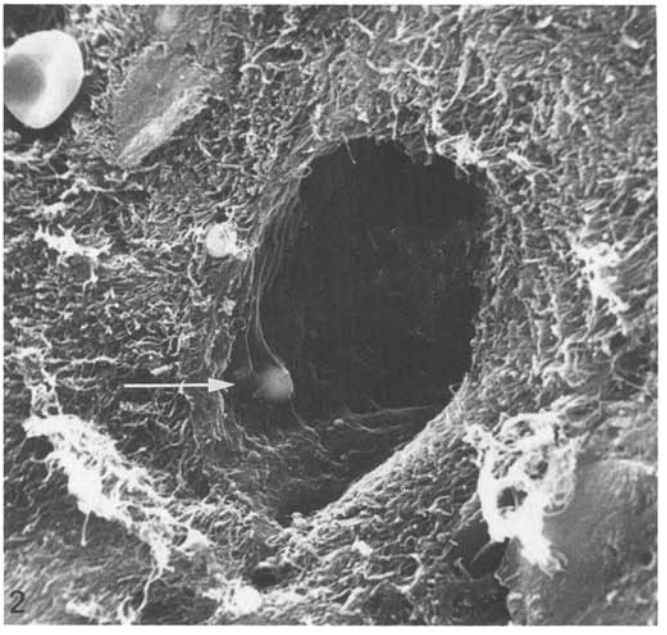

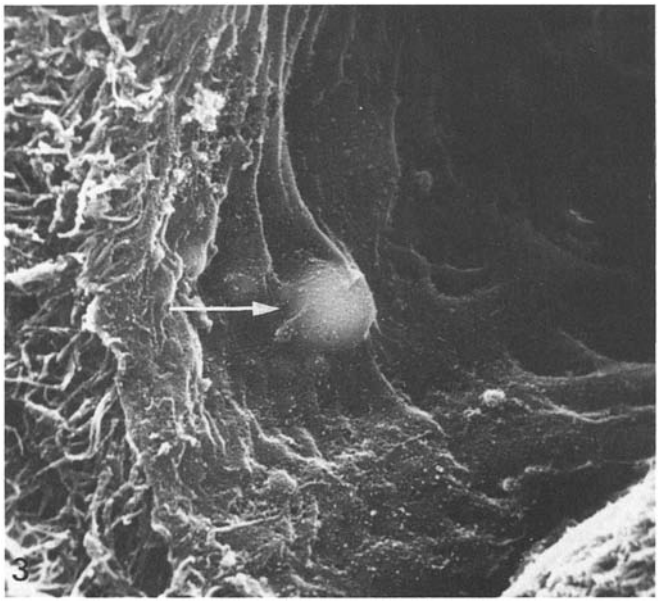

Fig. 1. Collecting duct near the papilla of a non stone bearing patient, *arrow* marks the microlith. Magnification 1,020:1, Calcium 3.4 x 10 – 3 mol/1, Oxalate 1.6 x 10 – 4 mol/l, saturation of calcium-ocalate 3.03

Fig. 2. Collecting duct near the papilla of a non stone bearing kidney, magnification 2,040:1, values of urine like Fig. 1

Fig. 3. Detail of Fig. 2, magnification 5,355:1, values of urine like Fig. 1. *Arrow* marks a microlith embedded in an oragnic matric

As crystallisation proceeded an increasing intratubular obstruction occurred (Fig. 11, 12). Calcium analysis by EDAX revealed that in a stone-free kidney crystal deposition did not only take place in the tubular lumen but also in the tubular wall. The corresponding EDAX point analysis showed (Fig. 10) a distinct peak beside the calcium peak (Fig. 13).

Chemical Analysis of Tissue Samples

Parallel to the morphological investigations the corresponding samples were chemically analysed. The kidney samples were wet mineralized followed by the determination of the concentrations of sodium, potassium, magnesium and zinc by flame atomic absorption spectroscopy (FAAS) (air;C_2H_2) and of calcium by FAAS (N_2O;C_2H_2). Cadmium, copper and lead were measured by anodic stripping voltammetry (ASV).

To ensure that the excised kidney samples were representative of the whole kidney, the distribution of the elements was examined in several kidneys. For this purpose the kidney samples were subdivided into cortex, medulla and papilla and then analysed. Figures 14–16 show the distribution of cadmium, calcium and magnesium in a tumor kidney. The black areas correspond to the highest concentration of a specific element. The segment used for the SEM analysis (Fig. 11, 12) is marked by an arrow.

Intrarenal elements differed greatly. There were not only differences in the elemental concentration of cortex, medulla and papillary tissue but also within the samples of a specific tissue. This distribution pattern for the different elements

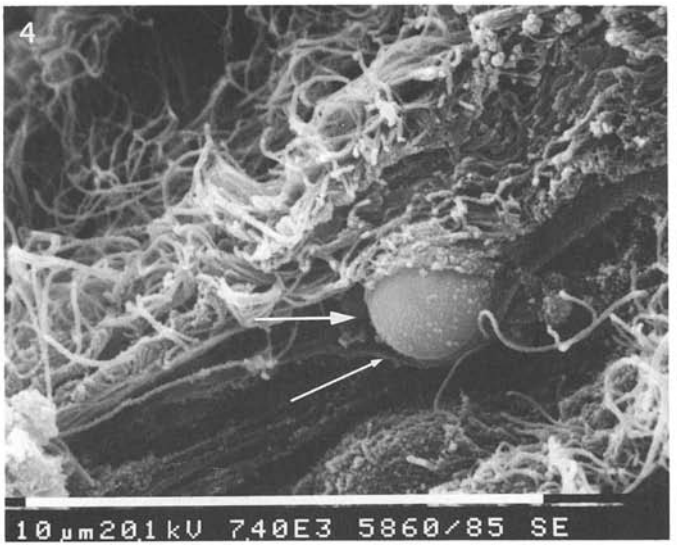

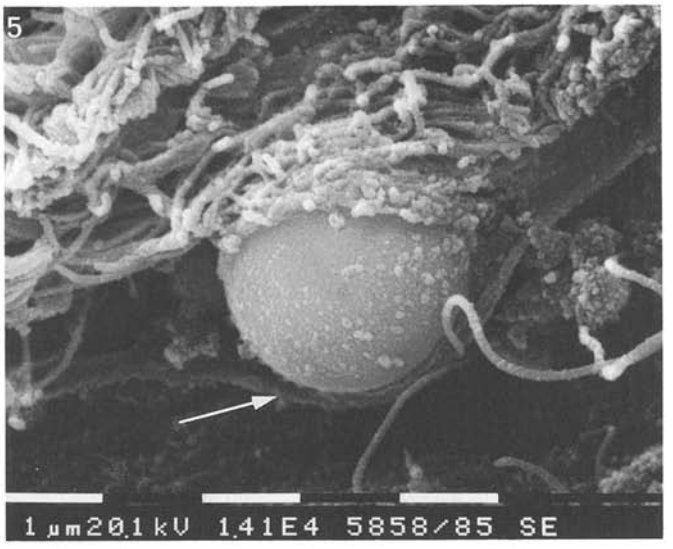

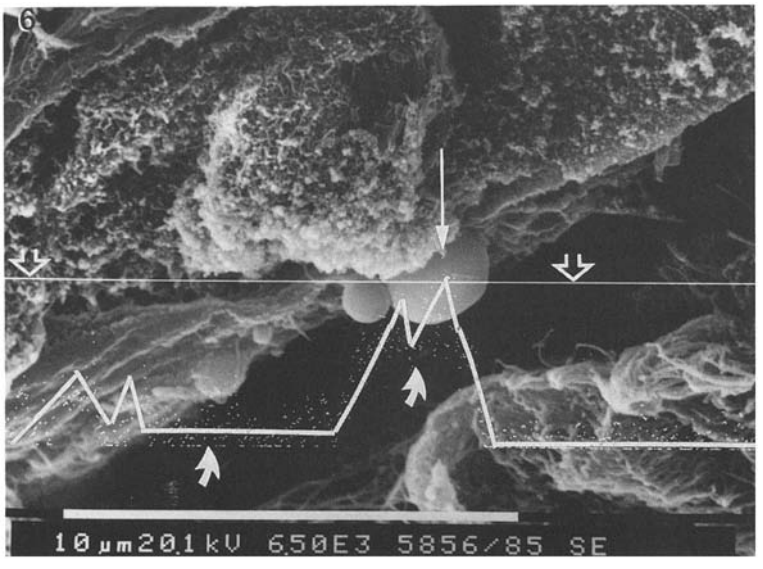

Fig. 4. Longitudinal section of a collecting duct of a stone bearing kidney. *Arrow* marks organic film embedding a microlith. Magnification 5,698 : 1

Fig. 5. Detail of Fig. 4. Magnification 10,857 : 1

Fig. 6. Longitudinal section of a collecting duct of a stone bearing kidney. *Small arrow* marks a crystall lying on the tubular epithelium. *White line* marks site of scan analysis for calcium (*open arrosw*). *Arrows* mark the result of calcium concentration. Magnification 5,005 : 1

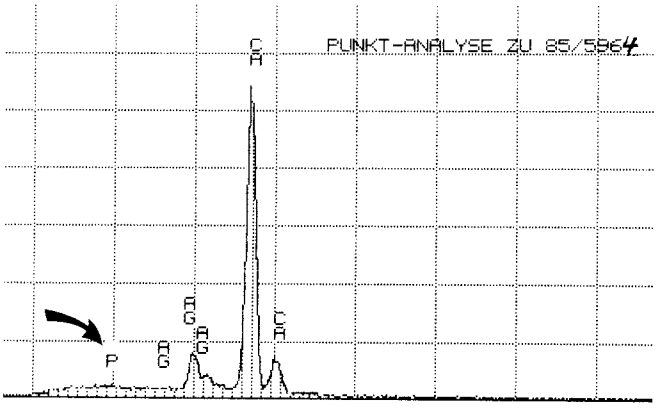

Fig. 7. Point analysis of the crystal from Fig. 6. There is only calcium and a very low phosphate peak (marked by *black arrow*) detectable

showed clearly that the composition of a single kidney sample is not representative of the total elemental content of a kidney [3, 4, 5].

The mean values for the distribution of the different elements in such a kidney showed high standard deviations but some tendencies were evident (Table 1).

- *sodium, potassium, magnesium, copper*

no significant differences between cortex, medulla and papilla

- *calcium*

concentration increases from cortex to papilla; within the papilla very high variations occurred

- *zinc, cadmium*

concentraion decreased from cortex to papilla

- *lead*

present only in a few samples,

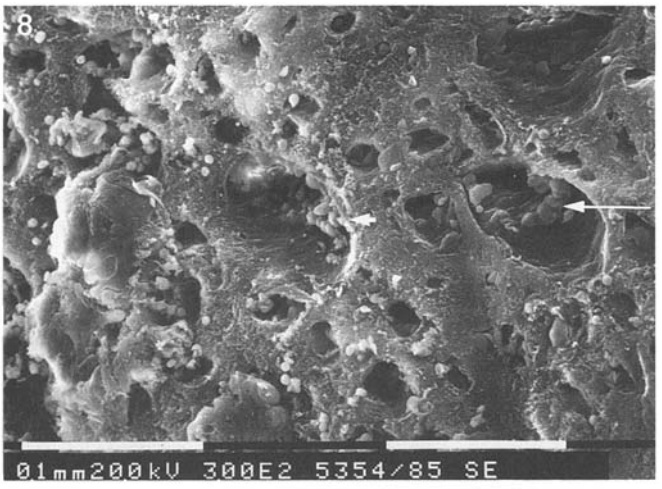

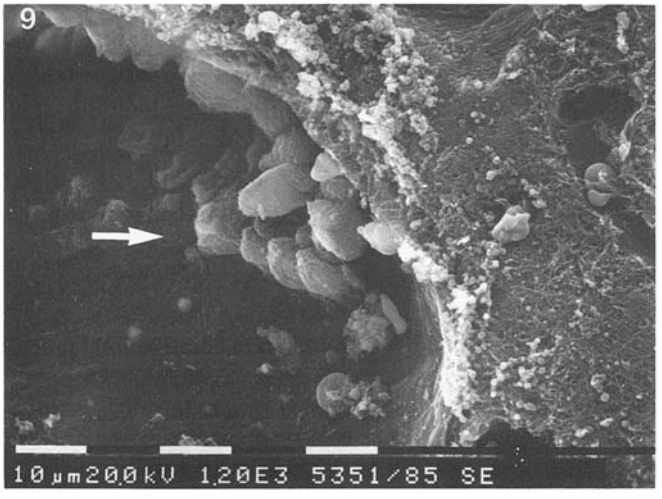

Fig. 8. Cross cut of a collecting duct of a non-stone bearing kidney. *Arrows* mark microliths lying on the tubular wall. Calcium 1.4 x 10 – 3 mol/l. Oxalate 0.3 x 10 – 4 mol/l and saturation of calcium oxalate 0.35. Magnification 198:1

Fig. 9. Detail of Fig. 8. Magnification 752:1. *Arrow* marks crystals arranged like cobble stones

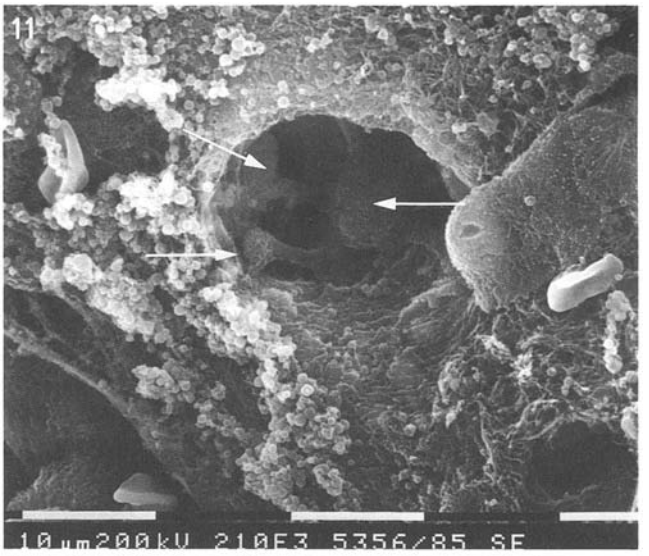

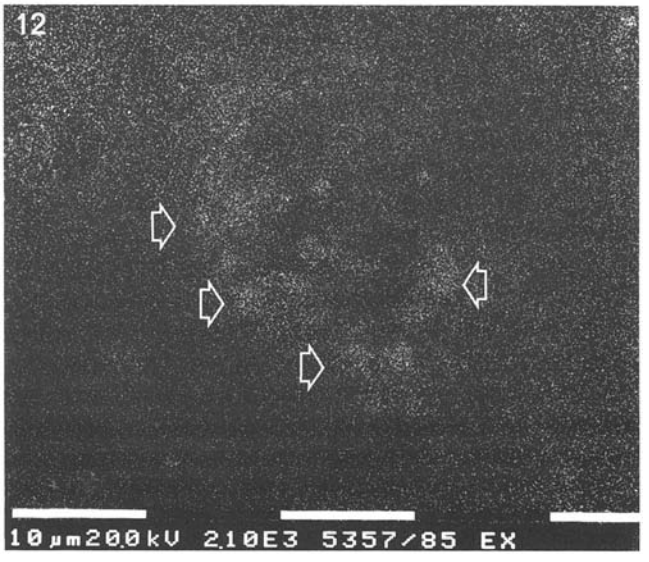

Fig. 11. Cross-cut of a collecting duct of a non-stone bearing kidney. The collecting duct is obstructed by intratubular crystals marked by *arrows*. Magnification 2,100:1, values of urine like Fig. 8

Fig. 12. Element distribution analysis of calcium. Magnification like Fig. 11. *Arrows* mark calcium spots located intratubularly and in the tubular wall

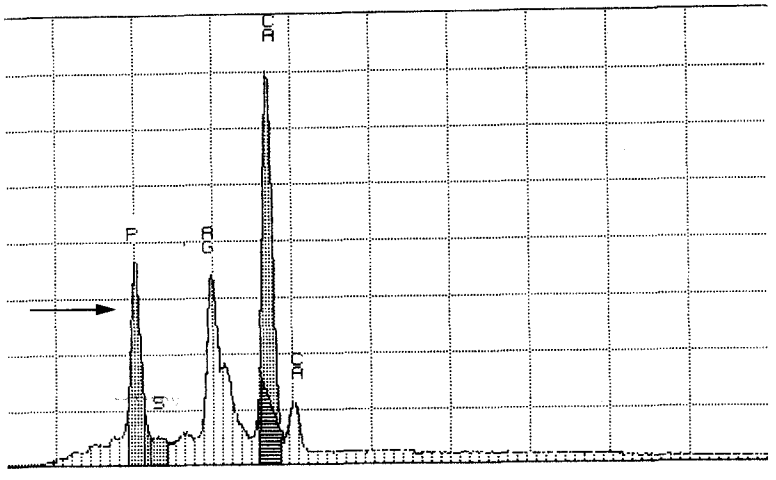

Fig. 10. Point analyses of a crystal in Fig. 9. In contrast to Fig. 7 there is a remarkably high phosphate peak

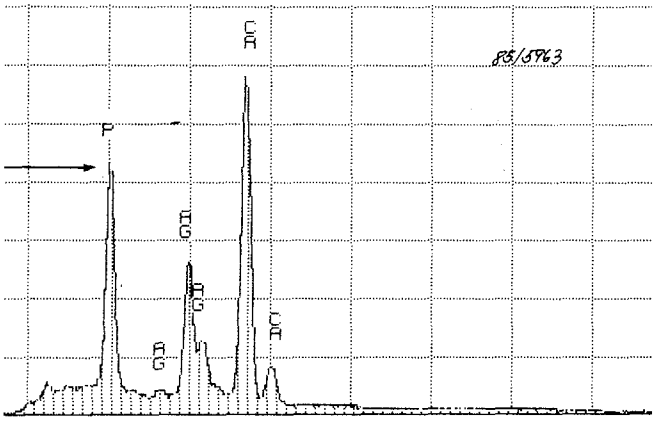

Fig. 13. Point analysis of the marked crystal in Fig. 11. *Black arrow* marks high phosphate peak

Table 1. Tissue concentrations of a tumour bearing kidney divided in cortex, medulla and papilla

	Cortex	Medulla	Papilla
Sodium (mg/g)	6.71 ± 0.72	8.21 ± 1.39	9.52 ± 2.34
Potassium (mg/g)	10.92 ± 0.73	10.71 ± 1.34	8.88 ± 1.48
Calcium (ppm)	1,336 ± 424	2,227 ± 701	5,606 ± 2,005
Magnesium (ppm)	746 ± 143	781 ± 201	839 ± 131
Zinc (ppm)	275 ± 105	173 ± 111	92 ± 51
Copper (ppm)	26 ± 9	23 ± 14	22 ± 17
Cadmium (ppm)	337 ± 137	103 ± 76	51 ± 59

All values refer to dry weight of the tissue samples

Fig. 14. Cadmium distribution of a tumour bearing kidney, stripe shaped samples containing cortex, medulla and papilla. *Black arrow* marks a stripe divided for chemical analysis and scanning electron microscopy

Fig. 15. Calcium distribution of a tumour bearing kidney like Fig. 14

Fig. 16. Magnesium distribution of a tumour bearing kidney like Fig. 14

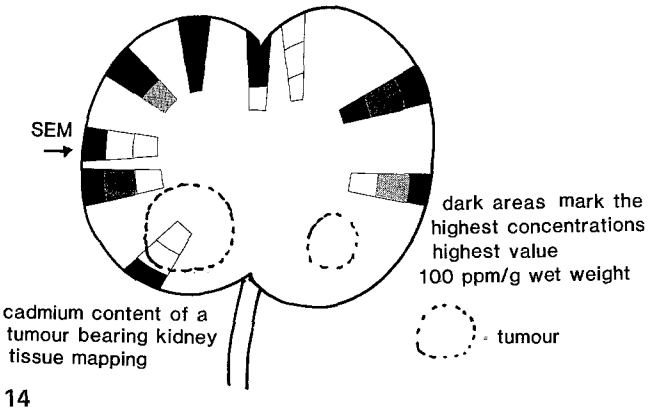

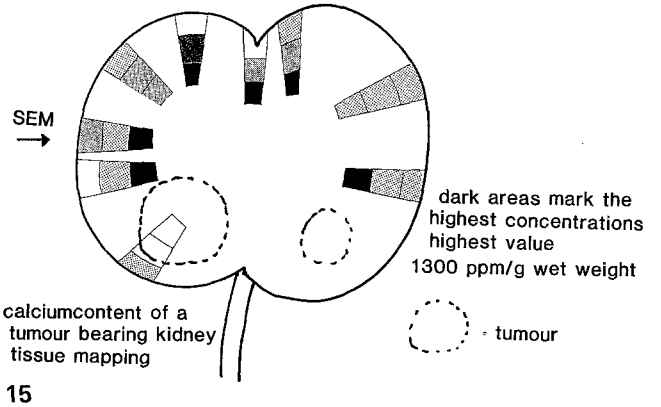

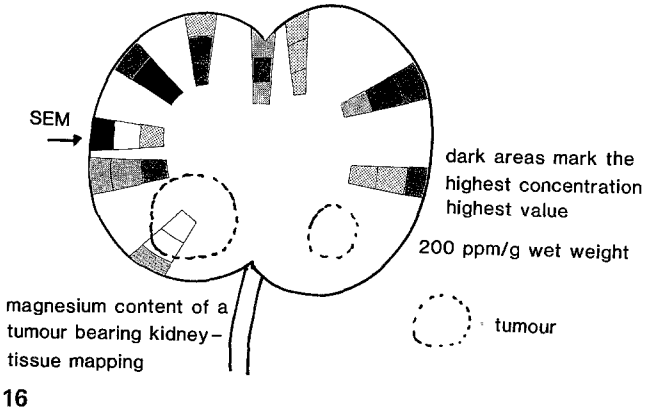

Table 2. Tissue concentration of non stone forming and stone forming kidneys divided in medulla, cortex and papilla

	Sodium in mg/g	Potassium in mg/g	Calcium in ppm	Magnesium in ppm	Zinc in ppm	Copper in ppm	Cadmium in ppm
Non stone formers							
Cortex	11.4 ± 6.2	9.5 ± 2.1	1,125 ± 809	707 ± 91	238 ± 31	14 ± 4	126 ± 81
Medulla	12.9 ± 2.4	9.1 ± 2.9	1,778 ± 1,385	648 ± 122	128 ± 55	17 ± 9	34 ± 46
Papilla	13.5 ± 5.0	8.8 ± 2.9	2,954 ± 2,361	694 ± 204	111 ± 53	13 ± 5	19 ± 29
Stone formers							
Cortex	10.2 ± 1.3	9.3 ± 2.8	1,102 ± 1,200	678 ± 107	214 ± 48	19 ± 8	103 ± 56
Medulla	16.2 ± 8.6	9.1 ± 2.8	1,964 ± 1,578	704 ± 107	162 ± 86	14 ± 11	36 ± 40
Papilla	12.1 ± 4.0	8.1 ± 2.9	3,524 ± 5,050	612 ± 301	113 ± 36	13 ± 6	23 ± 38

Table 3. Correlation of cadmium concentration in cortex, medulla and papilla to microlith formation in non stone forming and stone forming kidneys

	Microliths in SEM	Cd in cortex (ppm)	Cd in medulla (ppm)	Cd in papilla (ppm)	Ca in papilla (ppm)
Non stone formers					
1	–	51	31	18	492
2	–	19	80	4	1,391
3	–	102	3	7	8,882
4	+ (+ medulla)	199	167	11	1,047
5	–	69	7	4	3,081
6	+	325	120	39	936
7	+ (in tissue)	216	7	18	1,391
8	+	142	33	7	1,673
9	+	56	31	6	4,567
10	–	85	9	31	1,035
11	–	41	5	9	2,006
12	–	97	4	14	2,792
13	–	141	47	128	2,593
14	–	61	8	5	2,623
15	–	135	7	10	2,982
16	+	162	–	15	1,933
17	+	119	12	6	6,920
18	+	254	9	6	6,834
Stone formers					
1	+ (+ medulla)	161	103	19	852
2	–	30	1	1	1,054
3	+	120	64	3	1,829
4	+	162	27	114	213
5	–	29	8	1	1,223
6	+	108	93	58	3,893
7	+	169	8	8	16,483
8	–	54	9	<1	7,606
9	–	96	7	1	1,299
10	+	–	–	–	–

Table 4. Urine values of stone forming and nonstone forming kidneys

	Urine	
	Stone former	Non stone former
Supersaturation calcium oxalate (EQUIL)	5.03	1.61
Ca (mMol/l)	3.42	2.28
Oxalate (0.1 mMol/l)	1.16	0.54
Mg (mMol/l)	1.70	2.60
Citrate (0.1 mMol/l)	7.76	6.46

The high differences in element concentrations influence the mean values of all analysed kidney material. For this reason practically no differences between kidneys of stone formers and kidneys of patients free of stones was found (Table 2). We have confirmed the increasing concentrations of calcium from cortex to papilla and an inverse gradient for cadmium. The other elements showed no or negligable differences.

Discussion

It is well known that cadmium has nephrotoxic properties and the possibility of a connection between cadmium load and urolithiasis was discussed by Scott [6] in a long-term study.

Correlation of the morphological aspects of the SEM appearances and the results of the chemical analysis showed that 8 kidneys of the 18 stone-healthy and 6 kidneys of the 10 stone forming patients contained microliths. However, the corresponding papillary calcium concentrations showed no statistical differences. It is striking that in almost all kidneys with crystals the cadmium concentration of the corresponding cortex sample was increased. Equally the medullary samples with observed microcrystals yielded a significantly increased medullary cadmium content. Otherwise there was no statistically significant correlation between cadmium content and observed crystals in the papilla itself (Table 3).

The urine supersaturation with respect to calcium oxalate analysed by Finlayson's EQUIL 1 program [2] was found to be higher – 5.03 versus 1.61 – in the stone forming group.

Reasons for this effect were the higher calcium- and oxalate- as well as the lower magnesium excretion. However, the differences were not significant (high standard deviations) (Table 4).

References

1. Hering F, Lüönd G, Briellmann Th, Guggenheim H, Seiler H, Rutishauser G (1985) Frühformen von Harnsteinen in Humannieren – eine REM-Studie. In: Gasser G, Vahlensieck W (Hrsg) Pathogenese und Klinik der Harnsteine XI. Steinkopff, Darmstadt, S 282–289
2. Finlayson B (1977) Calcium stones, some physical and clinical aspects. In: David DJ (ed) Calcium metabolism in renal failure and nephrolithiasis. Wiley and Sons, New York, p 337
3. Hautmann R, Lehmann A, Komor S (1980) Calcium and oxalate concentrations in human kidney tissue – the key to the pathogenesis of stone formation. J Urol 123:317
4. Seiler HG (1986) Some problems encountered in the analysis of biological materials for toxic trace elements. In: Sigel H (ed) Met Ions Biol Syst, vd 20. Dekker, New York, pp 305–336
5. Wrigth RS, Hodgkinson A (1972) Oxalic acid, calcium and phosphorus in the renal papilla of normal and stone forming rats. Invest Urol 9:369
6. Scott R (1982) The importance of cadmium as a factor in calcified upper urinary tract stone disease – a prospective 7-year study. Br J Urol 42:584–589

Priv.-Doz. Dr. F. Hering
Urologische Klinik
Departement für Chirurgie
Universität Basel
Kantonsspital
CH-4031 Basel
Switzerland